Journal of Power Sources 195 (2010) 1046–1050

Contents lists available at ScienceDirect

Journal of Power Sources

journal homepage: www.elsevier.com/locate/jpowsour

Short communication

# Simple preparation of Pd–Pt nanoalloy catalysts for methanol-tolerant oxygen reduction

Wei He[a], Juanying Liu[b], Yongjin Qiao[b], Zhiqing Zou[b], Xiaogang Zhang[a], Daniel L. Akins[c], Hui Yang[b,*]

[a] College of Materials Science and Engineering, Nanjing University of Aeronautics and Astronautics, Nanjing 210016, PR China
[b] Shanghai Institute of Microsystem and Information Technology, Chinese Academy of Sciences, 865, Changning Road, Shanghai 200050, PR China
[c] CASI, The City University of New York, New York 10031, USA

ARTICLE INFO

*Article history:*
Received 15 July 2009
Received in revised form 2 September 2009
Accepted 2 September 2009
Available online 10 September 2009

*Keywords:*
Pd–Pt alloy
Oxygen reduction reaction
Complexing–reduction
Electrocatalysis
Methanol tolerance

ABSTRACT

Carbon-supported Pd–Pt bimetallic nanoparticles of different atomic ratios (Pd–Pt/C) have been prepared by a simple procedure involving the complexing of Pd and Pt species with sodium citrate followed by ethylene glycol reduction. As-prepared Pd–Pt alloy nanoparticles evidence a single-phase *fcc* disordered structure, and the degree of alloying is found to increase with Pd content. Both X-ray diffraction and transmission electron microscopy characterizations indicate that all the Pd–Pt/C catalysts possess a similar mean particle size of ca. 2.8 nm. The highest mass and specific activity of the oxygen reduction reaction (ORR) using the Pd–Pt/C catalysts are found with a Pd:Pt atomic ratio of 1:2. Moreover, all Pd–Pt alloy catalysts exhibit significantly enhanced methanol tolerance during the ORR than the Pt/C catalyst, ensuring a higher ORR performance while diminishing Pt utilization.



## 1. Introduction

The direct methanol fuel cell (DMFC), because of system simplicity and environmental friendliness, is a promising electrochemical energy converter for a variety of applications. For DMFCs, the oxygen reduction reaction (ORR) has been extensively studied because of its important role as the rate-determining reaction [1]. But several factors related to the ORR have hindered the commercialization of DMFCs. Examples include the high costs of Pt, slow kinetics, and crossover of methanol from the anode to the cathode. The latter leads to a "mixed potential" effect on the cathode side and decreases fuel efficiency.

To address the crossover problem, one strategy is the development of novel ORR electrocatalysts with high catalytic activity and good methanol tolerance. Novel Pd–Pt alloy catalysts might be promising candidates as methanol-tolerant ORR catalysts, because of the lower cost and greater abundance of Pd, as well as the lower reactivity observed for the Pd–Pt alloys towards methanol oxidation [2–4]. Moreover, compared with Pt–M (M: non-noble metal) catalysts, the utilization of Pd–Pt catalysts for cathodes avoids leaching out of the non-noble metal elements under electrochemical conditions because the long-term stability of Pd in acidic media is comparable with Pt [5,6]. Furthermore, it is to be noted that some reports have revealed that the ORR activity of binary Pt–Pd catalysts is superior to that of the Pt/C in DMFCs [7–9].

It is well known that the synthesis method has a strong influence on the composition, dispersion, morphology and the performance of catalysts. A complex reduction method that involves the complexing of metal salts followed by reduction has often been found to be the most effective approach for obtaining catalysts with small particle size and narrow size distribution. For instance, Li et al. [10] reported the preparation of the Pd/C catalysts of small particle size by a $NH_3$-mediated polyol route. However, due to the strong complex ability of $NH_3$ ligand, the complex Pd–$NH_3$ could not be reduced completely by ethylene glycol, and the post-treatment in a reductive atmosphere was needed. Also, Chen et al. [11] demonstrated that the formation of the complex between $H_2PtCl_6$ and THF leads to the onset reduction potentials of $H_2PtCl_6$ shifting in the negative direction.

For the bimetallic Pd–Pt catalysts for methanol-tolerant ORR, it is highly expected to prepare alloy nanoparticles with a very small particle size and a high alloying degree, which could be beneficial to an improvement in ORR activity and to a high methanol tolerance during the ORR [12,13]. In this paper, we sought to prepare carbon-supported Pd–Pt nanoalloy catalysts employing sodium citrate (SC) as complex agent, to decrease the reduction rate, thereby promoting desired monodispersed particle size and distribution. Meanwhile, the formation of complexes of Pd and Pt ions with SC would lead to co-reduction of Pd and Pt complexes, thus a well-alloyed Pd–Pt catalyst could be obtained. The

* Corresponding author. Tel.: +86 21 32200534; fax: +86 21 32200534.
*E-mail address:* hyang@mail.sim.ac.cn (H. Yang).

0378-7753/$ – see front matter © 2009 Elsevier B.V. All rights reserved.
doi:10.1016/j.jpowsour.2009.09.006

preparation method used here is quite simple and very efficient. The as-prepared Pd–Pt/C catalysts were characterized by various physical and electrochemical techniques. Also, the ORR activities and methanol tolerance of the Pd–Pt/C bimetallic catalysts were assessed.

## 2. Experimental

### 2.1. Catalyst preparation

Pd–Pt/C catalysts of different atomic ratios were synthesized by an ethylene glycol (EG) reduction route, with the aid of SC as the complexing agent. Briefly, palladium chloride [$PdCl_2$] and sodium hexachloroplatinate [$Na_2PtCl_6$] in EG were added to SC in EG solution. This mixture was stirred overnight to form the complexes, and the solution pH was adjusted to ca. 9–10. Subsequently, a calculated amount of XC-72R was dispersed in the solution, and the total metal loading was fixed at 20 wt.%. The suspension was maintained at a temperature of 140 °C under $N_2$ atmosphere for 4 h. After cooling to room temperature, the mixture was filtered, washed and dried overnight under vacuum at 70 °C. For a comparison, the Pd/C and Pt/C catalysts were also prepared under the same conditions.

### 2.2. Physical characterization

X-ray diffraction (XRD) measurements were conducted using a Rigaku D/MAX-2000 diffractometer with Cu $K_\alpha$ radiation. The tube voltage was maintained at 40 kV and tube current at 100 mA. Diffraction patterns were collected with a scanning rate of 2° $min^{-1}$ and with a step of 0.02°. The sample for transmission electron microscopy (TEM) analysis was prepared by ultrasonically suspending the catalyst powder in ethanol. A drop of the suspension was then placed onto a clean holey copper grid and dried under air. The morphology of the catalysts was characterized using a JEOL JEM 2100F operated at 200 kV.

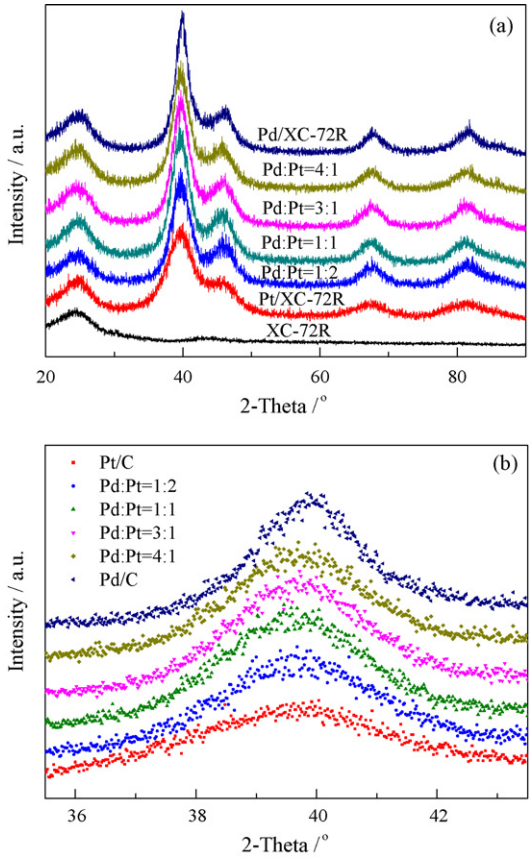


**Fig. 1.** XRD patterns of the Pt/C, Pd/C and Pd–Pt/C catalysts with various atomic ratios.

### 2.3. Electrochemical characterization

Electrochemical measurements were performed using a CHI 730 Potentiostat and a conventional three-electrode cell. The ORR activity was measured with a RDE mounted with a BM-ED 1101 electrode (Radiometer, France). Porous electrodes were prepared as follows: 10 mg of Pd–Pt/C alloy catalyst, 0.5 mL of Nafion (5 wt.%, Aldrich) and 2.5 mL of ultrapure water were mixed ultrasonically. Then, 3 μL of this ink was transferred onto a glassy carbon disk (GC, 3 mm diameter), and left to dry overnight. Each electrode contained ca. 28 μg $cm^{-2}$ of the metal. The counter electrode was a GC plate, and a saturated calomel electrode was used as the reference electrode. All potentials, however, are referenced with respect to the reversible hydrogen electrode (RHE). To determine the real electrochemical surface area (ECSA) of the Pd–Pt/C catalysts, CO stripping voltammetry was conducted. CO was pre-adsorbed at a potential of 0.05 V/RHE for 30 min by bubbling CO into 0.1 M $HClO_4$ solution, and CO dissolved in solution was subsequently removed by purging high-purity $N_2$ for 45 min. The ECSA was derived by integrating the $CO_{ad}$ oxidation area, after subtracting the background current in the CO stripping voltammograms, and assuming 420 μC $cm^{-2}$ as the oxidation charge of monolayer CO on a smooth Pt or Pd surface [14,15].

All experiments were carried out at a temperature of 25 ± 1 °C.

## 3. Results and discussion

### 3.1. Physical characterization of Pd–Pt/C catalyst

UV–vis spectra confirmed the formation of complexes of Pd and Pt species with SC after the mixture was stirred overnight at room temperature (data not shown) [16,17]. The complexing of Pd or Pt salts with SC decreases the reduction potential of the Pd or Pt species, which may be beneficial for the formation of Pd–Pt alloy catalysts with small particle size and good dispersion.

Fig. 1 shows the XRD patterns of as-prepared Pd/C, Pt/C and Pd–Pt/C alloy catalysts. The first peak located at ca. 24.8° in all the XRD patterns is ascribed to the carbon support. The other four peaks are characteristics of the face-centered-cubic (*fcc*) crystalline Pd, corresponding to the planes (1 1 1), (2 0 0), (2 2 0) and (3 1 1), respectively; indicating that all the catalysts are principally single-phase disordered structures (i.e., solid solutions). These four diffraction peaks for the Pd–Pt/C alloy catalysts located at the intermediate position between Pt/C and Pd/C catalysts. With the increase in Pd content within the Pd–Pt/C catalysts, these diffraction peaks shifted to higher $2\theta$ values, indicating decreased lattice parameters and high degree of alloying. The mean crystalline sizes of these catalysts are calculated based on the X-ray linewidths of (2 2 0) reflection using the Scherrer equation. The obtained particle sizes for different catalysts are provided in Table 1. Clearly, the Pd–Pt/C alloy catalysts of different Pd/Pt atomic ratios have the same *fcc* disordered structure and similar particle sizes (ca. 2.8 nm). The formation of the complexes of Pd and Pt ions with SC results in the co-reduction of metal ions and the alloying of Pd with Pt.

Fig. 2 shows two typical TEM images of the Pd–Pt/C alloy catalysts with Pd/Pt atomic ratio of 1:1 and 3:1, and their corresponding particle size distribution histograms. The Pd–Pt alloy nanoparticles are found to be well-dispersed on the surface of carbon with a narrow particle size distribution. Based on measuring the size of more

**Table 1**
XRD and electrochemical results of the Pd/C, Pt/C and Pd–Pt/C catalysts.

| Sample | Particle size (nm) | $S_{XRD}$[a] ($m^2\ g^{-1}$) | $ECSA_{CO}$ ($m^2\ g^{-1}$) | CO oxidation peak (V) | SA at 0.90 V $\mu A^{-1}\ cm^{-2}$ | SA at 0.85 V $\mu A^{-1}\ cm^{-2}$ |
|---|---|---|---|---|---|---|
| Pt/XC-72R | 2.4 | 116.55 | 62.07 | 0.739 | 3.54 | 24.6 |
| Pd:Pt = 1:2 | 2.7 | 114.26 | 40.08 | 0.745 | 6.27 | 39.7 |
| Pd:Pt = 1:1 | 2.8 | 118.29 | 42.45 | 0.787 | 3.64 | 29.5 |
| Pd:Pt = 3:1 | 2.9 | 132.75 | 48.64 | 0.832 | 1.01 | 17.5 |
| Pd:Pt = 4:1 | 2.8 | 143.14 | 54.34 | 0.838 | 2.14 | 12.0 |
| Pd/XC-72R | 3.0 | 166.67 | 42.13 | 0.860 | 2.13 | 1.7 |

[a] Calculated from the formula $S = 6000/\rho d$, where $\rho$ is the density of the alloy and $d$ is the average particle size (nm, XRD results).

than 200 randomly chosen particles in the TEM images, the mean particle sizes of the as-prepared Pd–Pt/C alloy catalysts are $2.8 \pm 0.2$ and $2.9 \pm 0.3$ nm, respectively; the values are in good agreement with the XRD results.

### 3.2. Electrochemical characterization of Pd–Pt/C catalyst

Fig. 3 shows the CO stripping voltammograms of the Pd/C, Pt/C and Pd–Pt/C catalysts. From the figure, it is clear that the onset and peak potentials of adsorbed CO oxidation on the Pd–Pt/C catalysts locate at the intermediate position between Pt/C and Pd/C catalysts. With the increase in Pd content within the Pd based catalysts, the onset and peak potentials of the $(CO)_{ad}$ oxidation are shifted to more positive potentials, suggesting that a well-alloyed Pd–Pt alloy was formed. The CO tolerance increases in the order of $Pt/C < Pd_1Pt_2/C < Pd_1Pt_1/C < Pd_3Pt_1/C < Pd_4Pt_1/C < Pd/C$, probably due to the effect of surface Pd/Pt composition of the catalysts. It is believed that the electron density transferring from Pd to Pt in the Pd–Pt alloys leads to a weakening and strengthening of CO band with Pd and Pt, respectively [18,19]. By integrating the $CO_{ad}$ oxidation area, the ECSA for each sample can be obtained and is listed in Table 1. With the increase in Pd content within the Pd–Pt bimetallic catalysts, the ECSA decreases in the same trend with the XRD-determined surface area ($S_{XRD}$). It is worth mentioning that adsorbed CO oxidation involves only a single peak on the Pd–Pt/C catalysts, suggesting that the oxidation peak is not simply an addition of fractional contributions of Pt and Pd sites and that a synergistic effect is evident.

A comparison of the ORR on the Pt/C, Pd/C and Pd–Pt/C alloy catalysts is provided in Fig. 4. The ORR activity decreases in the order of $Pd_1Pt_2/C > Pt/C \geq Pd_1Pt_1/C > Pd_3Pt_1/C > Pd_4Pt_1/C > Pd/C$; as indicated, and, interestingly, the ORR activity of the $Pd_1Pt_2/C$ is slightly enhanced compared with that for the Pt/C. Because of the similarity of the particle size and dispersity, the size effects on the catalytic activity were minimized, and the enhanced ORR activity may be ascribed to an optimal alloy composition as well as to a Pd–Pt synergistic effect [2,20].

Generally, the enhancement in specific activity (SA) of the ORR on Pt or Pd based alloy catalysts is correlated to the geometric and electronic change of the metal [21]. The change in SA of the

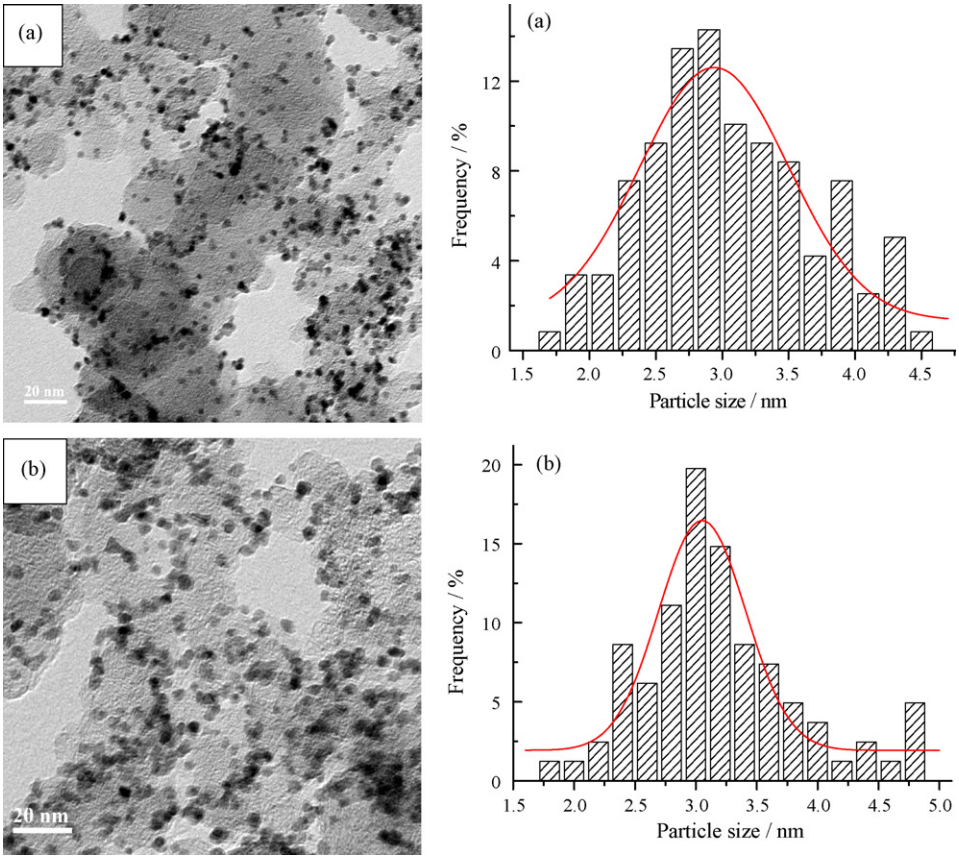


**Fig. 2.** Two typical TEM images of the Pd–Pt/C catalysts with Pd/Pt atomic ratios of (a) 1:1 and (b) 3:1.

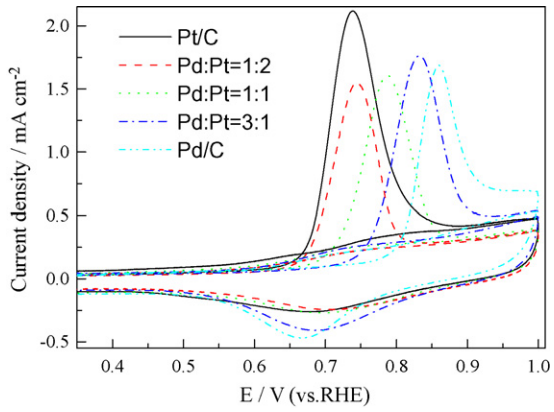


**Fig. 3.** CO stripping voltammograms of the Pd/C, Pt/C and Pd–Pt/C catalysts in 0.1 M $HClO_4$ after 30 min CO adsorption. Current densities are normalized to the geometric surface area.

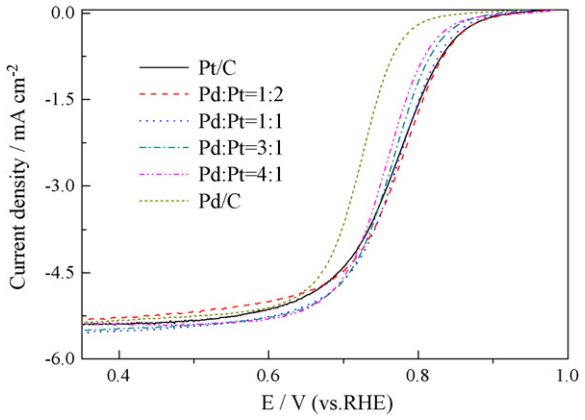


**Fig. 4.** Linear scan voltammograms (LSVs) of the Pt/C, Pd/C and Pd–Pt/C alloy catalysts in 0.1 M $HClO_4$ saturated with pure $O_2$ (5 mV $s^{-1}$ and 1600 rpm).

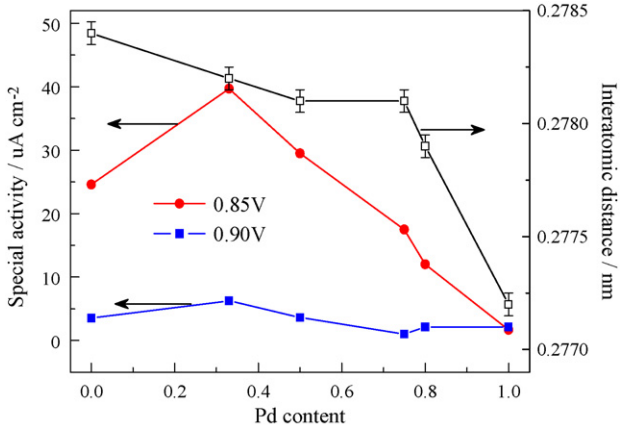


**Fig. 5.** The relationship between interatomic distance and specific activity at 0.90 and 0.85 V, respectively.

ORR at 0.90 and 0.85 V on the catalysts and the mean interatomic distance as a function of the Pd content are plotted in Fig. 5. A nearly monotonic correlation is observed between SA and interatomic distance expressed as a function of the Pd content within the Pd–Pt/C catalysts. The highest SA for the ORR was found with a Pd:Pt atomic ratio of 1:2. As reported, Norskov et al. [22,23] initially proposed that the catalytic activity of the metals can be rationalized in terms of the energy of d-band center ($\varepsilon_d$). With an upshift of $\varepsilon_d$, a distinctive anti-bonding state appears above the Fermi level. For these states are empty ones, a strong bonding takes place. Conversely, weak bonding occurs if they are shifted down through the Fermi level (and become filled). Through the shifting of $\varepsilon_d$, one can raise or lower the activity of metal catalysts. Adzic and co-workers [21,24–26] deposited a monolayer of Pt on metal substrates via galvanic displacement of a previous underpotential deposition of Cu monolayer for electrocatalytic purposes. They extended the Norskov model to interpret the enhancement of methanol oxidation reaction and ORR activities on Pt monolayer. Due to the mismatch in the lattice constants between the Pt monolayers and their substrates, a tensile or compressive force is generated, which entails a variation in the width of the d-band, thereby shifting its center to preserve the degree of d-band filling. Thus, for Pt monolayer deposited on different substrates, there would be a volcano-type dependence of ORR activity on $\varepsilon_d$. Compressive strain tends to downshift $\varepsilon_d$ in energy, weakening Pt–$O^-$ adsorption, and so enhancing the ORR kinetics of Pt monolayer. On the other hand, tensile strain tends to narrow the Pt d-band, with an upshift in $\varepsilon_d$, leading a stronger Pt–$O^-$ adsorption. Tegou et al. [27] also prepared stable Pt- and Au-coated Fe, Co, Ni and Pb deposits on glassy carbon electrodes. They proposed that the changes in $\varepsilon_d$ might be responsible for the ORR activities on different metals, where a lowering of $\varepsilon_d$ is associated with a decrease in metal chemisorption affinity towards O, CO, H and other adsorbates. With respect to the Pd–Pt alloys, a synergistic effect [2,20] was reported due to the fact that Pd and Pt have a similar ORR behavior. A slight but strong $\varepsilon_d$ downshift and oxygen bond weakening can further improve the catalytic activity of Pt for the ORR. Li et al. [5] observed a significantly enhanced ORR activity on the $Pt_3Pd_1$/C catalyst as compared with that for Pt, and showed the charges are transferred from the *d* orbital of Pd to the *s* and *p* orbitals of Pt by density function theory calculation. In our work, the addition of Pd in the Pd–Pt/C catalyst induces the changes in the Pt–Pt distance and the metal d-band energy center as a result of the smaller atom radius of Pd than that of Pt and the electronic contribution of Pd, modifying the catalytic properties of metal. Thus, it is believed that the improvement in the ORR kinetics on the $Pd_1Pt_2$/C catalyst is ascribed to a decreased Pt-Pt interatomic distance and to a lowered Pt $\varepsilon_d$ [28], arising from alloying of Pt with Pd.

As is known, the crossover of methanol from the anode to the Pt cathode can lead to a further reduction in cell voltage, by ca. 200–300 mV. There is a competitive reaction between oxygen reduction and methanol oxidation on Pt-based cathodes. Therefore, it is highly desirable to develop selective-ORR electrocatalysts that have a high methanol tolerance for DMFC applications. Fig. 6a shows the ORR performances on Pt/C and Pd–Pt/C alloy catalysts in the presence of 0.5 M $CH_3OH$ solution at a scan rate of 5 mV $s^{-1}$ and a rotating speed of 1600 rpm in order to evaluate the ORR activity in the methanol-containing electrolyte. As compared to the ORR in pure $HClO_4$ solution, the catalysts exhibited an increase in overpotential under the same current density in the presence of methanol. The methanol oxidation peaks is found to become increasingly smaller with increase in Pd content. Furthermore, Fig. 6b shows the LSVs of the P/C, Pd/C and Pd–Pt/C catalysts in 0.1 M $HClO_4$ + 0.5 M $CH_3OH$ saturated with pure $N_2$ at a scan rate of 5 mV $s^{-1}$. From the figure, it can be seen that the current densities of the methanol oxidation reaction on the Pd based catalysts are much lower than that on the Pt/C catalyst, indicating that the alloy catalysts for methanol oxidation are less active than the Pt/C catalyst. The current densities of the methanol oxidation reaction increase with Pt content within the Pd–Pt alloy catalysts. In fact, a comparison of Fig. 6a and b clearly shows that a higher reactivity of methanol oxidation corresponds to a lower ORR activity on all the catalysts at different polarization potentials. This observation is consistent with the fact

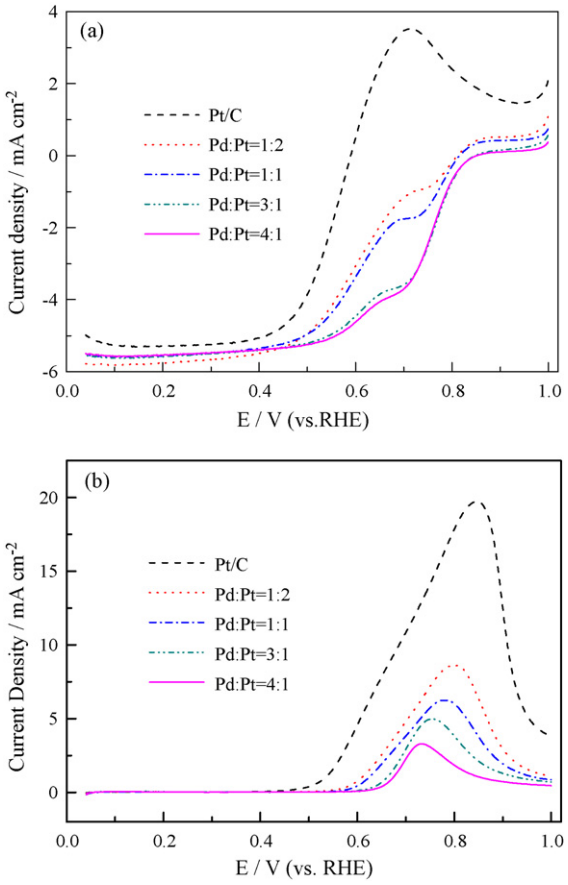


**Fig. 6.** LSVs of the Pt/C and Pd–Pt/C catalysts with different atomic ratios in 0.1 M $HClO_4$ + 0.5 M $CH_3OH$ saturated with pure $O_2$ (a) and $N_2$ (b), respectively.

that Pd is inactive for methanol oxidation in acidic solution and the dissociative chemisorption of methanol requires the existence of at least three adjacent Pt ensembles [29,30], which is influenced by the presence of Pd atoms around the Pt active sites that are expected to block methanol adsorption on Pt sites due to the dilution effect.

## 4. Conclusions

In summary, we prepared carbon-supported Pd–Pt nanoalloy catalysts with different atomic ratios via a complex reduction involving SC. The Pd–Pt alloy nanoparticles are found to be well-dispersed on the surface of carbon with a small particle size (ca. 2.8 nm) and a very narrow particle size distribution. Also, the as-prepared Pd–Pt alloy catalysts show comparable ORR activity with Pt/C catalyst as well as a good methanol tolerance during the ORR. Due to its simplicity and efficiency, this SC-complexing reduction method for the synthesis of highly active Pd–Pt nanoalloy catalysts might be easily scaled for industrial production.

## Acknowledgments

We would like to thank the NSF of China (20673136 and 20706056), the National "863" Programs of China (2007AA05Z141 and 2008AA05Z102) and the 100 People Plan Program of CAS for support of this work. DLA, additionally, would like to thank the U.S. NSF for support primarily by the Nanoscale Science and Engineering Initiative under Award Number CHE-0641523, and by the New York State Office of Science, Technology, and Academic Research (NYSTAR).

## References

[1] A.B. Anderson, J. Roques, S. Mukerjee, V.S. Murthi, N.M. Markovic, V. Stamenkovic, J. Phys. Chem. B 109 (2005) 1198–1203.
[2] W.M. Wang, Q.H. Huang, J.Y. Liu, Z.Q. Zou, Z.L. Li, H. Yang, Electrochem. Commun. 10 (2008) 1396–1399.
[3] Z.W. Chen, M. Waje, W.Z. Li, Y.S. Yan, Angew Chem. Int. Ed. 46 (2007) 4060–4063.
[4] L. Jiang, A. Hsu, D. Chu, R. Chen, J. Electrochem. Soc. 156 (2009) B370–B376.
[5] H.Q. Li, G.Q. Sun, N. Li, S.G. Sun, D.S. Su, Q. Xin, J. Phys. Chem. C 111 (2007) 5605–5617.
[6] H. Yang, N. Alonso-Vante, J.M. Leger, C. Lamy, J. Phys. Chem. B 108 (2004) 1938–1947.
[7] H. Li, Q. Xin, W. Li, Z. Zhou, L. Jiang, S. Yang, G. Sun, Chem. Commun. (Camb) (2004) 2776–2777.
[8] Y.H. Cho, B. Choi, Y.H. Cho, H.S. Park, Y.E. Sung, Electrochem. Commun. 9 (2007) 378–381.
[9] B. Lim, M. Jiang, P.H.C. Camargo, E.C. Cho, J. Tao, X. Lu, Y. Zhu, Y. Xia, Science (2009) 1170377–1170383.
[10] H.Q. Li, G.Q. Sun, Q.A. Jiang, M.Y. Zhu, S. Sun, Q. Xin, Electrochem. Commun. 9 (2007) 1410–1415.
[11] Y. Chen, Y.W. Tang, C.P. Liu, W. Xing, T.H. Lu, J. Power Sources 161 (2006) 470–473.
[12] J.B. Joo, Y.J. Kim, W. Kim, N.D. Kim, P. Kim, Y. Kim, J. Yi, Korean J. Chem. Eng. 25 (2008) 770–774.
[13] X.W. Li, Y. Zhu, Z.Q. Zou, M.Y. Zhao, Z.L. Li, Q. Zhou, D.L. Akins, H. Yang, J. Electrochem. Soc. 156 (2009) B1107–B1111.
[14] X.G. Li, I.M. Hsing, Electrochim. Acta 51 (2006) 3477–3483.
[15] H. Meng, S. Sun, J. Masse, J. Dodelet, Chem. Mater. 20 (2008) 6998–7002.
[16] S.H.Y. Lo, Y. Wang, C. Wan, J. Colloid Interf. Sci. 310 (2007) 190–195.
[17] J.W. Guo, T.S. Zhao, J. Prabhuram, C.W. Wong, Electrochim. Acta 50 (2005) 1973–1983.
[18] D.C. Papageorgopoulos, M. Keijzer, J.B.J. Veldhuis, F.A. de Bruijn, J. Electrochem. Soc. 149 (2002) A1400–A1404.
[19] R.M. Navarro, B. Pawelec, J.M. Trejo, R. Mariscal, J.L.G. Fierro, J. Catal. 189 (2000) 184–194.
[20] J. Zhang, Y. Mo, M.B. Vukmirovic, R. Klie, K. Sasaki, R.R. Adzic, J. Phys. Chem. B 108 (2004) 10955–10964.
[21] M.H. Shao, K. Sasaki, R.R. Adzic, J. Am. Chem. Soc. 128 (2006) 3526–3527.
[22] J.K. Norskov, J. Rossmeisl, A. Logadottir, L. Lindqvist, J.R. Kitchin, T. Bligaard, H. Jonsson, J. Phys. Chem. B 108 (2004) 17886–17892.
[23] J. Greeley, J.K. Norskov, M. Mavrikakis, Annu. Rev. Phys. Chem. 53 (2002) 319–348.
[24] R.R. Adzic, J. Zhang, K. Sasaki, M.B. Vukmirovic, M. Shao, J.X. Wang, A.U. Nilekar, M. Mavrikakis, J.A. Valerio, F. Uribe, Top. Catal. 46 (2007) 249–262.
[25] M.H. Shao, T. Huang, P. Liu, J. Zhang, K. Sasaki, M.B. Vukmirovic, R.R. Adzic, Langmuir 22 (2006) 10409–10415.
[26] M.B. Vukmirovic, J. Zhang, K. Sasaki, A.U. Nilekar, F. Uribe, M. Mavrikakis, R.R. Adzic, Electrochim. Acta 52 (2007) 2257–2263.
[27] A. Tegou, S. Papadimitriou, S. Armyanov, E. Valova, G. Kokkinidis, S. Sotiropoulos, J. Electroanal. Chem. 623 (2008) 187–196.
[28] J.H. Yang, J.Y. Lee, Q.B. Zhang, W.J. Zhou, Z.L. Liu, J. Electrochem. Soc. 155 (2008) B776–B781.
[29] J.J. Wang, G.P. Yin, G.J. Wang, Z.B. Wang, Y.Z. Gao, Electrochem. Commun. 10 (2008) 831–834.
[30] J. Salgado, E. Antolini, E.R. Gonzalez, Appl. Catal. B: Environ. 57 (2005) 283–290.